

Effect of the Shape Factor as an Input Variable on the Extraction Process for a Reversing Continuous Countercurrent Extractor

Waigoon RITTIRUT¹ and Chairat SIRIPATANA²

¹*School of Agricultural Technology, Walailak University, Nakhon Si Thammarat 80161, Thailand*

²*School of Engineering and Resources Management, Walailak University, Nakhon Si Thammarat 80161, Thailand*

(Corresponding author; e-mail: rwaigoon@wu.ac.th)

Received: 28th July 2010, Revised: 26th October 2010, Accepted: 16th November 2010

Abstract

The effect of the shape factor on a reversing continuous countercurrent extraction process for concentration profiles is reported. Garcinia fruit was selected as a model solid while sucrose was used as soluble solid for the diffusion system. The results showed that a slab shape gave better results on the concentration profiles for both solid and liquid phases than those of the block shape. A better diffusion mass transfer in the slab shape leads to a better yield. The shape factor results were verified using a model solid system. The phenomena in reversing continuous countercurrent extraction process under steady-state conditions can be explained via a backmixing-diffusion model. The concentration profiles by model prediction corresponded well to those of measured data. Diffusivities which are available for simulation purposes were reported for different thicknesses and operating temperatures. The evaporation took place at an acceptable level for an open system according to the specified operating conditions.

Keywords: Garcinia fruit, *Garcinia atroviridis*, shape factor, countercurrent extraction, reversing extractor, backmixing-diffusion, concentration profile

Introduction

Continuous countercurrent diffusion (CCD) including extraction and infusion is widely used in the food and chemical industries. For juice production, the reversing continuous countercurrent extractor (RCCE) was one of the few technological breakthroughs in CCD. The unit was invented by Casimir (1983) under the cooperation project between the Commonwealth Scientific and Industrial Research Organization (CSIRO) of Australia and Bioquip Australia Pty Limited [1]. It was an effective instrument which was applied to the beverage juice concentrate industry [2]. The RCCE is a single screw unlike the more common type of double screw extractor, the De Danske Sukkerfabriker (DDS) diffuser [3].

The RCCE unit has been demonstrated to have potential for high yield of soluble solids, flavors and colors from wide ranging materials. A test run with apples, pears, and oranges in

comparison to the mechanical press, showed that the unit gave a higher yield of total soluble solid, a better juice quality and less suspended solid after purification [1]. It was reported that, based on the higher soluble solid yield, the CCD method was better than the traditional mechanical press [4]. Better economics in investment and operating cost were also shown by Emch [5], who studied juice production from apples and pears with plant capacity of 5 tons/h for a work season of 13 five day weeks operating 24 h per day.

However, for the single screw extractor which rotates continuously in one direction like the RCCE, the contact between the solid and liquid is not efficient as solids tend to ride up one side of the trough while the liquid flows relatively unimpeded down the other. The impaction pressure due to the screw rotation is continuous and uniform which also inhibits efficient contact

between the liquid and solids. CSIRO overcomes these problems by rotating the screw intermittently in reverse. The screw operated with more forward than backward rotation results in a net forward movement of solids, resulting in efficient solid-liquid contact [6].

The operation scheme of the RCCE process involves a number of input variables (factors and parameters) which must be considered in order to obtain a better yield (the required output and solutes). These variables include draft of extraction (corresponding to solid to liquid ratio), solid retention time, extraction time, operating temperature, degree of inclination (slope of the trough), external mass transfer resistance (corresponding to overall mass transfer coefficients and diffusivities), solvent selection, type, size and shape of raw materials, degree of backmixing of the solid and liquid phase (corresponding to percent forward progression and other movement and vibration), liquid hold up, and others [7].

This work follows previous work where the effect of the degree of inclination and percent forward progression by the net movement of screw conveyor were already reported [8]. Two different shape factors based on characteristic length, mass transfer area and volume of solid materials will be studied through a model solid where shrinkage or volume change during diffusion time does not play a major role. Although work has been reported for this factor for many kinds of agricultural materials, [1,3,9-12] these systems used solids where the shrinkage effect was negligible (not reported) as it was previously verified that the selected model solid possessed a rigid enough structure [13,14]. Here we have selected garcinia fruit as a model solid as the volume change is less than 2 % [14]. Hence, in this study the results will be due entirely to the shape factor as an input variable.

For the diffusion system, water and garcinia fruit were selected as liquid and solid phases, respectively; and to obtain a unique initial concentration before running each system, the diffusion of sucrose into the solid phase was scrutinized instead of the inherent soluble compounds like the hydroxycitric acids (HCA).

Materials and methods

Batch Diffusion

Fresh unripe garcinia fruits (*Garcinia atroviridis*), spherical in shape and green in color, were purchased locally in Nakhon Si Thammarat, Thailand. The unpeeled fruit were cut with a meat slicer into infinite slabs to the required thickness of ~2, 4 and 6 mm. The diameter of each circular slab material was in the range of ~7 - 10 cm. All materials were immersed in 0.06 % (w/v) calcium chloride for 6 h to maintain their firmness, drained for 30 min on a screen and then immersed in 60 % (w/v) sucrose solution (white, food grade) for a certain period (approximately 6 h) until an initial sugar concentration of 30 ± 3 °Brix was reached. The materials were kept at 4 °C with a relative humidity of 75 % RH in a controlled atmosphere until being used.

The diffusion experiments were carried out by batch extraction over a period of 3 h. The effect of operating temperature and thickness of the prepared materials (2, 4 and 6 mm) were investigated. Temperatures in the vessel (water bath) were varied at 50, 55, 60 and 70 °C. Each experiment was performed in triplicate.

For each treatment, the ratio of water to raw material was 30:1 (w/w). Stirring was continuous to maintain a turbulent flow to get rid of external resistance to mass transfer. Samples of the solid phase were taken at 2, 4, 6, 8, 10, 15, 20, 40, 70 and 180 min, respectively. Soluble solid content in the solid sample was determined with an Abbe Refractometer. The moisture content of the solid phase at the end of each experiment was also determined. The purpose of each diffusion experiment was to establish solute diffusivity (mainly sucrose) which was calculated with analytical solutions based on Fick's second law of unsteady-state diffusion, developed by Siripatana for symmetrical solids [15]. The equation was also mentioned in our previous work [14].

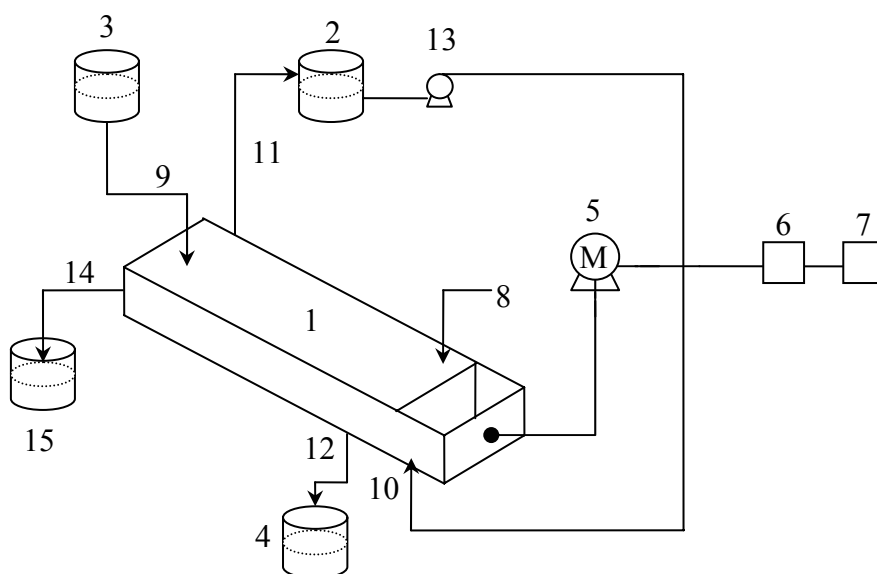
Continuous Countercurrent Diffusion

To investigate the effect of the shape factor on the concentration profile, two different shapes were studied: a slab 2 mm-thick and a block with dimensions of $7.5 \times 7.5 \times 7.5$ mm. The garcinia fruits were cut into the required shape before immersing in 60 % sucrose solution until an initial sugar concentration of 30 ± 3 °Brix was reached. All materials were then drained for 30 min before kept at 4 °C with a relative humidity of 75 % RH until being used for CCD experiments.

A reversing continuous countercurrent extractor (RCCE) with a 2 m long extraction chamber was used as the instrument. A schematic view is illustrated in **Figure 1** [8]. The solid phase was fed at the lower end of the trough where the relative length (z) was 0 (feeding position). The entering liquid phase was introduced at the other higher end where the relative length (z) was 1.

For each shape, the experiments were run in triplicate. The conditions for the RCCE process were fixed as follows:-

- the operating temperature was 55 °C
- the draft of extraction was 1.6
- the slope of the extraction unit was 5°
- percent forward progression by the screw conveyer was 10 %
- solid retention time was 55 min
- extraction time was 6 h



- 1 the Extraction barrel or trough
- 2 the Vessel of hot water circulated in a jacket around the trough
- 3 the Vessel of water, the entering liquid phase, fed into the extractor
- 4 the Vessel for juice collection, the extract phase accumulation
- 5 the Motor for rotating the screw shaft
- 6 the Inverter
- 7 the Microcomputer
- 8 the Area for feeding new solid raw materials at the lower end of the trough, relative length (z) = 0
- 9 the Area for feeding the entering liquid phase, at the higher end of the trough, relative length (z) = 1
- 10 the Hot water inlet to the jacket
- 11 the Hot water outlet from the jacket
- 12 the Juice outlet, the accumulated extract phase
- 13 the Pump for hot water circulation in the jacket around the trough
- 14 the Extraction point of solid raw materials from the trough
- 15 the Vessel for collection of extracted solid raw materials

Figure 1 Schematic view of the RCCE [8].

For each run, 6 kg of garcinia fruit were initially fed and fully distributed along the length of the extraction chamber. Further fruit was then added at a rate 0.5 kg for every 5 min (6 kg/h) until the total operation time (the extraction time) of 6 h was reached. The fruit was feed at the lower end of the extraction unit and at the end of the reversing cycle of the screw conveyer. Samplings were taken every 20 min for the first 3 h and then every 30 min for another 3 h (thus 6 h in total). Sample collections were done for both liquid and solid phases at each point along the extractor length. The relative length z (sampling position relative to the total length of the extraction trough) was 0.1, 0.3, 0.5, 0.7, 0.9 and 1.0, respectively.

Concentrations of soluble solids (mainly sucrose) for both the liquid and solid phase were determined using an Abbe Refractometer. The degree of soluble solid concentrations ($^{\circ}\text{Brix}$) was reported and the determination was also converted to kg/m^3 of occupied volume. The shape factor was calculated using planimeter for surface area and picnometer for volume and density measurement (liquid replacement method). Overall volumetric mass transfer coefficients were evaluated for each run according to Eq. (8) in reference [14]. Concentrations for both phases were converted to kg/m^3 of occupied volume.

Results and discussion

Diffusivity Evaluation of Soluble Solids from Batch Diffusion Process

Diffusivity was calculated based on Eq. (1) as follows [14]:

$$E = \frac{\bar{x} - x^*}{\bar{x}_0 - x^*} = \frac{\bar{y} - y^*}{y_0 - y^*} = \sum_{n=1}^{\infty} C_n \exp[-q_n^2 \tau]; \quad \tau = \frac{Dt}{a^2} \quad (1)$$

where

E is the remaining fraction of the extractable solute.

\bar{x} , \bar{x}_0 , x^* are the average, initial and equilibrium concentrations of the solute in the solid phase, respectively.

\bar{y} , y_0 , y^* are the average, initial and equilibrium concentrations of the solute in liquid phase, respectively.

q_n are the eigenvalues.

C_n is a series coefficients obtained by solving the equation of the eigenvalues.

τ is Fick's number.

D is the solute diffusivity.

a is the characteristic length; and

t is the time of diffusion.

The diffusivity is a mass transfer parameter and is available for simulation purposes. As shown in reference [14], only the linear portion was selected for diffusivity calculations. The selected range of time was 0 - 1,200 s since the concentration of the liquid phase did not interfere with the mass transfer. The higher the temperature, generally the higher the diffusivity (**Table 1**). Nevertheless, thickness also influenced the mass transfer since in the case of 4 and 6 mm thick-slabs as the temperature increased the diffusivity did not increase (**Table 1**).

At constant temperature the greater the thickness, the lower the diffusivity. The reason is maybe due to interactions between the internal solid structure of the materials and the solute components and also the inhomogeneity of the selected agricultural materials. The internal tissue structure and various components are responsible for diffusivity [16,17]. It was interesting to note that diffusivities for the 2 mm-slab were obviously higher than that of the 4 and 6 mm slabs while there is a little difference between 4 and 6 mm slabs (**Table 1**). Our results support those of others who claimed that thicknesses beyond 3 mm did not greatly influence the diffusivity [17,18].

All batch diffusion experiments in this work are actually to determine diffusivities. According to diffusion theory [3,10,16], the block shape is just the compounded superposition of 3 infinite slabs. Thus, it is not necessary to estimate diffusivity using block-shape material since theoretically diffusivity is the property of material depending its internal structure and thickness [18]. The main reason for the influence of thickness on diffusivity is the surface injury due to cutting which is more significant as the slab gets thinner.

Table 1 Solute (sucrose) diffusivities in the model solid at different slab thickness and temperature.

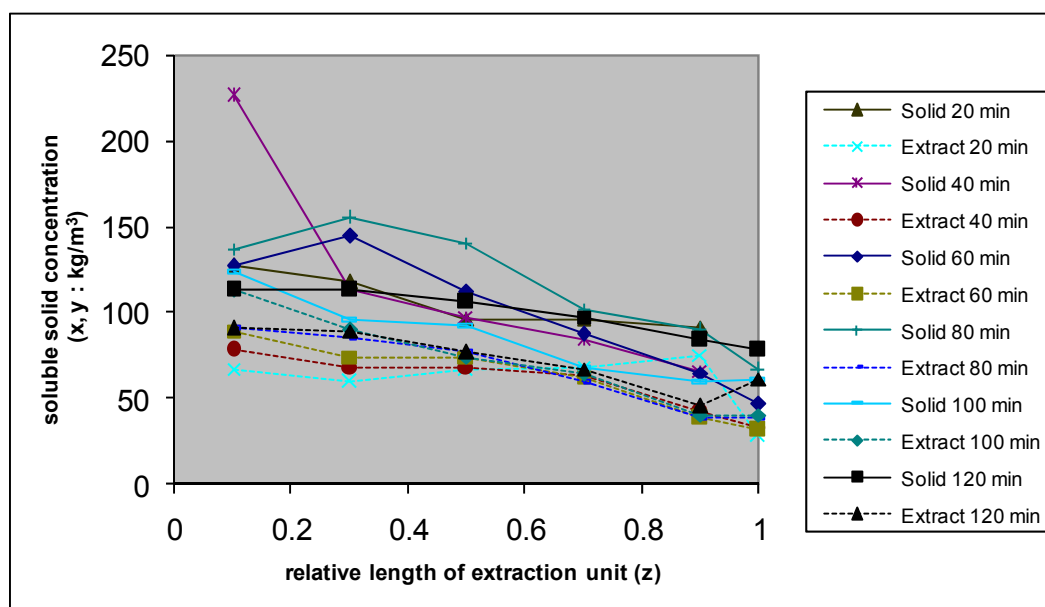
Temperature (°C)	Thickness (mm)	Solute diffusivity ($D \text{ (m}^2/\text{s)} \times 10^{-10}$)
50	2	2.29
	4	0.98
	6	0.66
55	2	2.95
	4	0.87
	6	0.75
60	2	3.28
	4	0.82
	6	0.71
70	2	3.60
	4	1.02
	6	1.00

Concentration Profile during Continuous Countercurrent Diffusion Process

In order to obtain constant diffusivity for each experiment, the temperature was controlled by circulating hot water in a jacket around the trough. The liquid phase density and solid phase moisture before and after extraction were also determined. For total 6 h operation, four final values of soluble solid concentration of both the

liquid and solid phase were averaged. For the purpose of this discussion, only the concentration profiles for each slab shape are presented. The results for other shapes have similar trends and are not presented here for brevity. In addition, any clear outliers were removed to simplify data analysis and discussion.

The solid phase concentration profile gradually decreased while the liquid phase gradually increased over time (**Figures 2 - 4**) due to gradual transfer of solid to the liquid phase. In the early extraction period especially during the first few hours, a lot of fluctuation in the concentration profiles was observed (**Figure 2**) (notable unsteady-state period). For sucrose diffusion, the system seemingly approached steady-state conditions after 3 - 4 h (**Figure 3**). Nevertheless, to assure that actual steady-state conditions were reached, only data collected during 5 - 6 h (**Figure 4**) were further used for considering the shape factor effect. It was observed that in every case, the solid concentration profile was more unstable than that of the liquid. The average concentration profile where steady-state conditions were reached is also presented in **Figure 5**.

**Figure 2** Solid and liquid (extract) phase concentration along the extraction unit for the slab shape treatment, 1 - 2 h (sampling time 0 - 120 min).

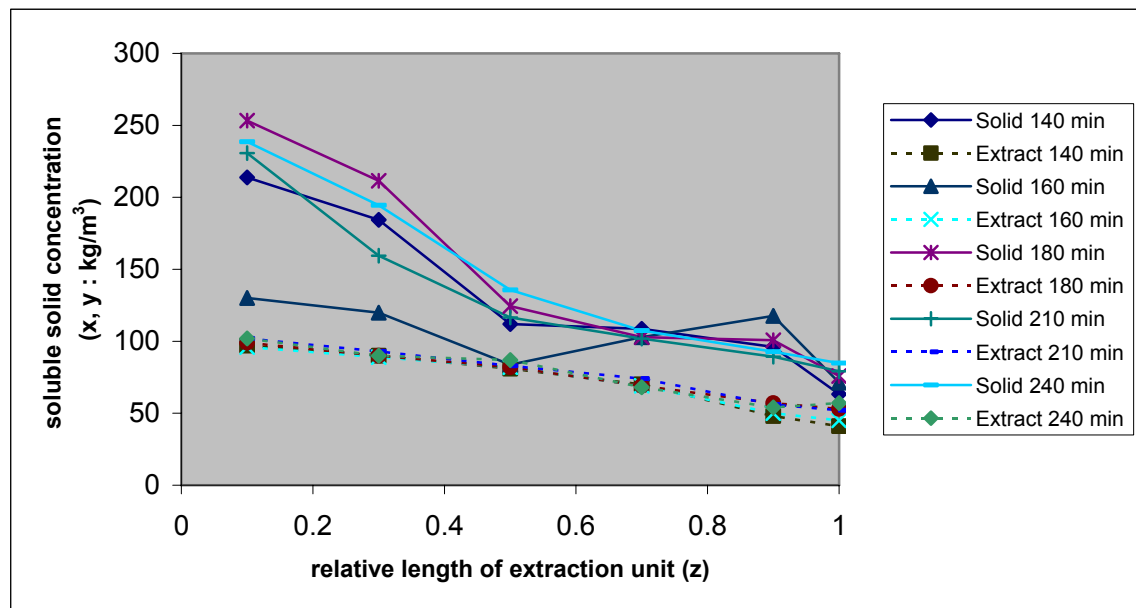


Figure 3 Solid and liquid (extract) phase concentration along the extraction unit for the slab shape treatment, 3 - 4 h (sampling time 140 - 240 min).

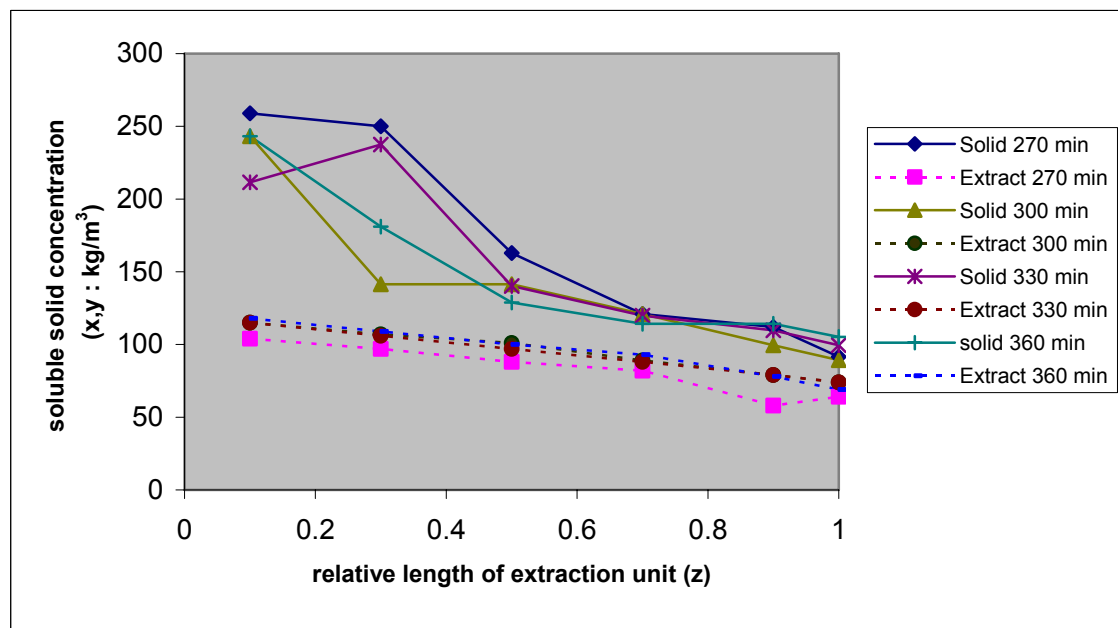


Figure 4 Solid and liquid (extract) phase concentration along the extraction unit for the slab shape treatment, 5 - 6 h (sampling time 270 - 360 min).

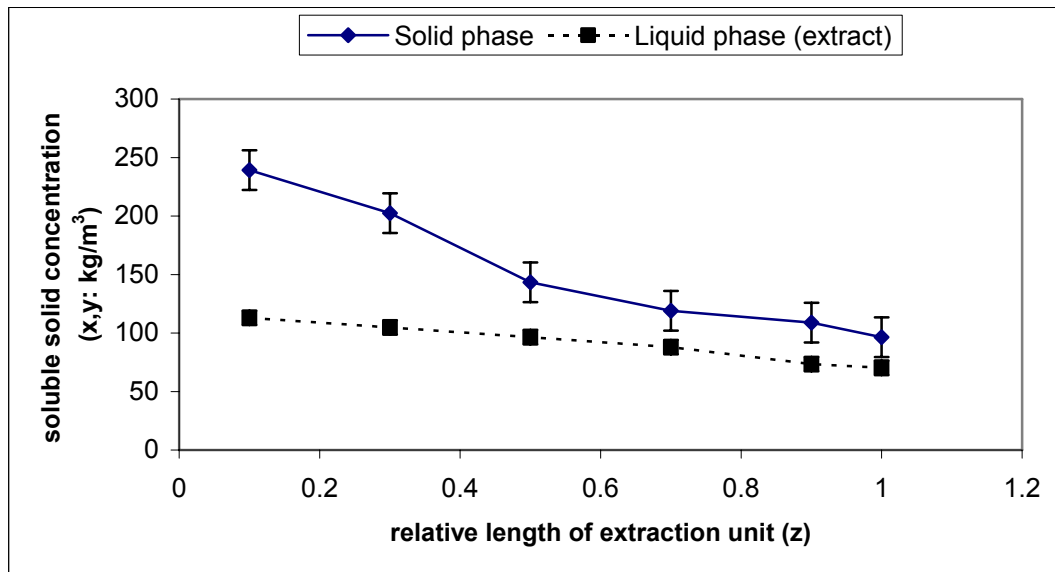


Figure 5 Average concentration profile for the solid and liquid (extract) phase along the extraction unit for the slab shape treatment, 5 - 6 h (sampling time 270 - 360 min).

Effect of Shape on Concentration Profile, Yield and Evaporation

The shape factor (ν) was calculated by Eq. (2) and is similar to Schwartzberg's work [3]. The effect of shape on the concentration profile for the solid and liquid phases is shown in **Figures 6** and **7**, respectively. The slab materials in this case have a diameter of at least 7 cm, hence may be considered as infinite slabs [16]. It was clearly observed that the slab shape (2 mm-thick, $\nu=1$) yielded better results for both liquid and solid phases in comparison to that of the block shape ($7.5 \times 7.5 \times 7.5$ mm, $\nu=3$). The reason was due to the larger surface area of mass transfer to the unit volume [3,9,15]. A better yield is also found (**Table 2**). Based on conventional shapes, diffusion mass transfer in an infinite slab ($\nu=1$) was higher than that of an infinite cylinder ($\nu=2$) and sphere ($\nu=3$) [19], and a block ($\nu=3$) in this case.

$$\text{shape factor } (\nu) = \frac{\text{characteristic length } (a) \cdot \text{mass transfer area } (A)}{\text{solid volume } (V)} \quad (2)$$

Table 2 Evaporation (% *evp*) and extraction yield* (% yield) as a percentage of the diffusion experiments for the RCCE open system.

Operating parameter	Parameter value/ characteristics	% <i>evp</i>	% yield
Shape of Raw material	Infinite slab	4.7	77.51
Shape of Raw material	Block	4.1	68.20

*extraction yield was calculated based on no evaporation

The percentage of evaporation (% *evp*) was determined based on an overall operating system by Eq. (3) while extraction yield was based on Eq. (4). Evaporation was due to the condition of the surrounding air for the open system and the screw movement. It is noted that the yield can also be calculated directly from the solid phase where the evaporation in this phase can be considered negligible [8].

$$\% \text{ evap} = \frac{(S_0 + L_0) - (S_f + L_f)}{(S_0 + L_0)} \times 100 \quad (3)$$

where S and L represent the solid and liquid flow rate, respectively, while the subscripts 0 and f correspond to the inlet and outlet of the extractor, respectively.

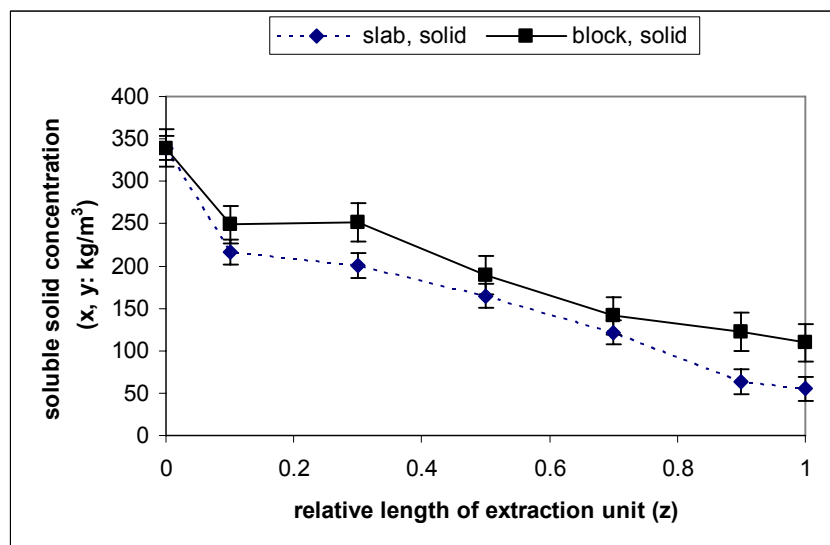


Figure 6 Effect of shape on the solid phase concentration profile at different points along the extractor under steady-state conditions.

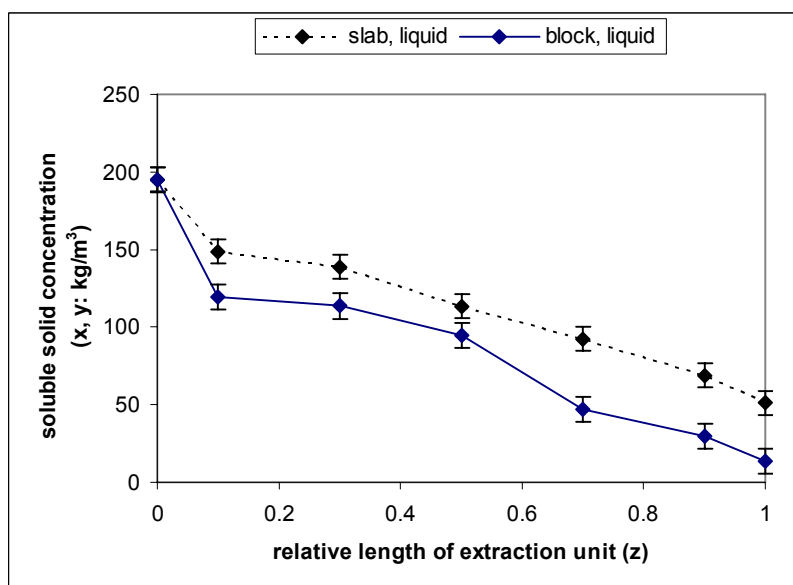


Figure 7 Effect of shape on the liquid phase concentration profile at different points along the extractor under steady-state conditions.

$$\% \text{ yield} = \frac{(x_0 - x_f)}{x_0} \times 100 = \frac{\alpha y_f}{m x_0} \times 100 \quad (4)$$

where α is the draft of extraction, m is the equilibrium distribution, x and y represent the solute concentration in the solid and liquid phase, respectively, while the subscripts 0 and f are for the inlet and outlet of the extractor, respectively.

Concentration Profile based on Backmixing-Diffusion Model

A backmixing-diffusion model is appropriate for describing phenomena in a continuous countercurrent extraction (CCE) system [20,21]. The concept can be generally applied to the RCCE system with similar boundary conditions. The model was proposed for solid and liquid phase using Eq. (5) and (6), respectively.

$$-\frac{\partial x}{\partial z} + \frac{\partial}{\partial z} \left(\frac{1}{P} \frac{\partial x}{\partial z} \right) - T_s (x - y/m) = \frac{\partial x}{\partial \theta} \quad (5)$$

$$\frac{\partial y}{\partial z} + \frac{\partial}{\partial z} \left(\frac{1}{\nu R} \frac{\partial y}{\partial z} \right) + T_L (x - y/m) = \frac{\nu S}{L} \frac{\partial y}{\partial \theta} \quad (6)$$

In addition, for Eq. (5)

$$\theta = t/\tau \text{ where}$$

$$\tau = \nabla_x / S \text{ and } t = \text{operation time}$$

$$z = \nabla_x / \nabla_x$$

$$P = \nabla_x S / D_x = \text{Peclet number in the solid}$$

phase

$$T_s = \frac{\nabla_x}{S} \frac{K_s dA}{dv_x} = \tau k_a$$

$$k_a = \frac{K_s dA}{dv_x} = \text{volumetric overall mass}$$

transfer coefficient (s^{-1})

In addition, for Eq. (6)

$$\nu_y = \nu \nu_x \text{ and } \nu = L/S$$

$$R = \nabla_x L / D_y = \text{Peclet number in the liquid}$$

phase

$$T_L = \frac{\nabla_x}{L} \frac{K_s dA}{dv_x} = T_s \frac{S}{L}$$

where,

$$S = \text{volumetric flow rate of solid phase (m}^3/\text{s)}$$

L = volumetric flow rate of liquid phase (m^3/s), as a function of time t

x = solute concentration in solid phase, as a function of time t and ∇_x (or z) (kg/m^3)

y = solute concentration in liquid phase, as a function of time t and ∇_x (or z) (kg/m^3)

∇_x = accumulated volume of solid phase from its inlet point to position considered (m^3)

∇_y = accumulated volume of liquid phase from its inlet point to position considered (m^3)

∇_x = total volume of solid phase in extraction unit

D_x = axial dispersion coefficient in solid phase (m^6/s), as function of t and ∇_x

D_y = axial dispersion coefficient in liquid phase (m^6/s), as function of t and ∇_x

K_s = overall mass transfer coefficient (m/s), a parameter depending on solute diffusivity D_s , came from diffusion theory

dA = area of mass transfer in volume $d\nabla_x$ (m^2)

x^* = average solute concentration in solid phase at equilibrium condition (kg/m^3)

y^* = solute concentration in liquid phase at equilibrium condition (kg/m^3)

The boundary conditions of Eq. (5) and (6) are as follows:

$$x_{in} = x - \frac{1}{P} \frac{\partial x}{\partial z} \text{ at } z = 0 \quad (7)$$

$$y_{out} = y, \quad \frac{1}{\nu R} \frac{\partial y}{\partial z} = 0 \text{ at } z = 0 \quad (8)$$

$$y_{in} = y + \frac{1}{\nu R} \frac{\partial y}{\partial z} \text{ at } z = 1 \quad (9)$$

$$x_{out} = x, \quad \frac{1}{P} \frac{\partial x}{\partial z} = 0 \text{ at } z = 1 \quad (10)$$

where

x_{in} and y_{in} are the solute concentrations in the solid and liquid phase at inlet of the extractor, respectively.

x_{out} and y_{out} is the solute concentration in the solid and liquid phase at outlet of the extractor, respectively.

The initial conditions are as follows:

$$x = 0, y = 0 \text{ for } 0 \leq z \leq 1 \text{ at } t = 0 \quad (11)$$

A solution to the model was proposed by Rittirut *et al* using a numerical method [20,21]. Simulation of the concentration profiles was conducted in a similar way as shown in that work. For the slab shape, the results are illustrated in **Figure 8** while for the block materials results are shown in **Figure 9**. Parameters for simulation were concluded in **Table 3**. Diffusivity for the block shape came from what was obtained by 4 mm-thick slab materials with an operating temperature of 55 °C (**Table 1**); This value was used by approximation using the method described by other researchers [7,9,12].

According to **Table 3**, α is the draft of extraction, τ is the solid retention time, m is the equilibrium distribution coefficient, P and R are Peclet numbers for the solid and liquid phase, respectively. x_{in} and y_{in} represent the solute concentration in the solid and liquid phase at inlet condition. k_a is the overall volumetric mass transfer coefficient (from diffusion theory), D_s is solute

diffusivity, a is characteristic length, j is factor for time of plasmolysis, Δz and $\Delta \theta$ are the relative length and time interval for numerical calculations previously [20,21].

It was clearly shown that backmixing-diffusion model well corresponded to actual data at steady state condition (**Figures 8** and **9**), corresponding to what was concluded in the previous work [20,21]. It was interesting to note that parameters like the P , R and j -factors were adjusted until the predictions were mostly close to the measured data. The quite low value of Peclet number for liquid phase ($R = 4$) implied that the system were shifted to mixed flow condition for a certain level. The degree of backmixing for liquid phase was obviously higher than that of solid phase ($R < P$). All j values were lower than 1.0 (**Table 3**) which implied that the surface washing took effect as soon as the solid materials were in contact with the liquid phase [15,22].

Table 3 Parameters and constants for prediction by backmixing-diffusion model to obtain concentration profile for the solid and liquid phase for the slab and block shapes.

Parameters and constants	Figure 8	Figure 9
Raw materials	garcinia fruit	garcinia fruit
Solid shape	slab	block
Solid flow rate (kg/min)	0.125	0.125
Solid density (kg/m ³)	1035.0	1035.0
Slope of extractor	5°	5°
Operation time (min)	360	360
α	1.6	1.6
τ (min)	55	55
x_{in} (kg/m ³)	339.3	339.3
y_{in} (kg/m ³)	0	0
m	1.07	1.07
P	10	10
R	1.3	4
k_a (s ⁻¹)	0.0005233	0.000385
D_s (m ² /s)	2.95×10^{-10}	0.87×10^{-10}
$2a$ (mm)	2.0	7.5
j	0.8	0.86
Δz	0.1	0.1
$\Delta \theta$	0.01	0.01

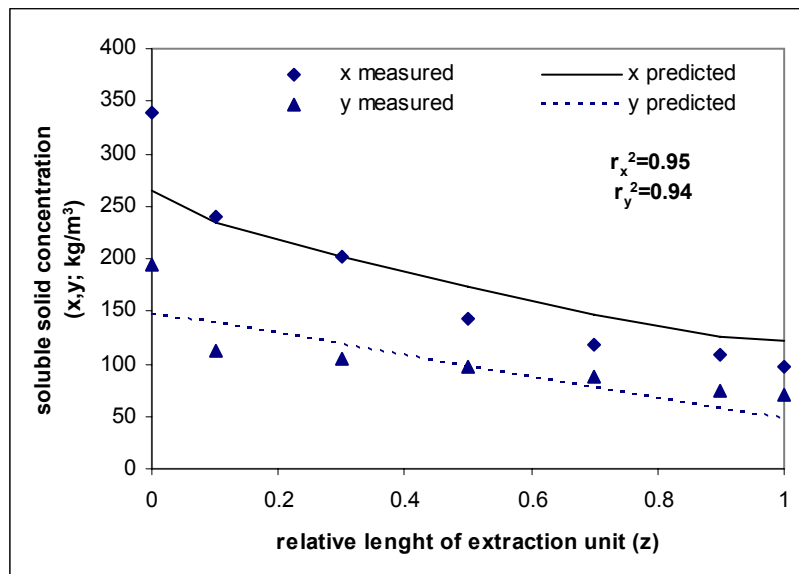


Figure 8 Measured and predicted concentration for the solid (x) and liquid (y) phase along the length of the extraction unit under steady state conditions (operating time of 360 min) for the slab shape treatment (2 mm-thick slab material).

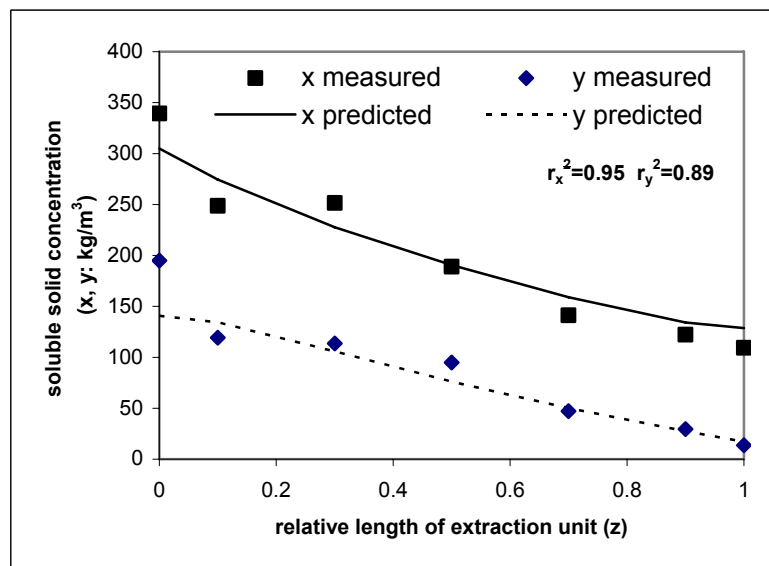


Figure 9 Measured and predicted concentration for the solid (x) and liquid (y) phase along the length of the extraction unit under steady state conditions (operating time of 360 min) for the block shape treatment ($7.5 \times 7.5 \times 7.5 \text{ mm}^3$).

Conclusions

The higher the temperature, the higher the sucrose diffusivity generally obtained. Thickness influenced the mass transfer to a certain extent. At constant temperature, the greater the thickness, the lower the diffusivity. The diffusivities in 2 mm-slabs were obviously higher than that of 4 and 6 mm slabs while there is nearly no difference between 4 and 6 mm-slabs.

The influence of the shape factor on concentration profile was clear with a lower shape factor resulting in a better concentration profile in both the liquid and solid phase. The block shape is inferior to the slab shape in term of diffusion mass transfer, leading to a lower yield. The results were verified by a model solid system. Evaporation rates were normal compared to other RCCE open systems.

Based on a backmixing-diffusion model, the simulation of the concentration profile was successful under steady-state conditions. Hence the transport mechanism can be explained by backmixing-diffusion. The model was then verified in this case.

Acknowledgements

The authors wish to thank the Institute of Research and Development, Walailak University and the Energy Policy and Planning Office, Ministry of Energy, Thailand for supplying research funds.

References

- [1] DJ Casimir. Counter current extraction of soluble solids from foods. *CSIRO. Food Res. Quar.* 1983; **53**, 38-43.
- [2] AJ Jones. A chronology of Australian bioscience, chemical and chemical engineering achievements: part I (1976 - 2006). In: *Chemistry in Australia*, March, 2007, p. 7-17.
- [3] HG Schwartzberg. Continuous counter current extraction in the food industry. *Chem. Eng. Prog.* 1980; **76**, 67-85.
- [4] CR Binkley and RC Wiley. Continuous diffusion-extraction method to produce apple juice. *J. Food Sci.* 1978; **43**, 1019-23.
- [5] F Emch. *Extraction of fruit and vegetables*. In: *Food Process Engineering*. App. Sc. Pub. Ltd., London, 1980, p. 424-33.
- [6] S Gunasekeran, RJ Fisher, and DJ Casimir. Predicting soluble solids extraction from fruits in a reversing, single screw countercurrent diffusion extractor. *J. Food Sci.* 1989; **5**, 1261-5.
- [7] W Rittirut. 2009, Modeling simulation of solid-liquid diffusion in continuous countercurrent extraction process, Ph.D. Thesis. Walailak University, Thailand.
- [8] W Rittirut and C Siripatana. Effect of some operating parameters on the reversing continuous countercurrent extraction process. *Walailak J. Sci. & Tech.* 2009; **6**, 203-15.
- [9] C Siripatana. 1986, Mass transfer in a reversing countercurrent extractor. Master of Applied Science Thesis. University of New South Wales, Australia.
- [10] HG Schwartzberg. *Leaching organic materials*. In: Ronald W. Rousseau (ed.). *Handbook of separation process technology*. John Wiley & Sons, Inc. New York, 1987, p. 540-77.
- [11] YC Lee and HG Schwartzberg. *Effect of Axial Dispersion During Solid-Liquid Extraction*. In: WEL Spiess and H Schubert. (eds.). *Engineering and Food volume III*. Elsevier Science Publishers, London, 1990, p. 1-10.
- [12] T Thummadetsak. 1996, Mass transfer in pineapple juice extractor. Master of Engineering Thesis (*in Thai*). Prince of Songkla University, Songkhla, Thailand.
- [13] W Rittirut and C Siripatana. Drying characteristics of *Garcinia atroviridis*. *Walailak J. Sci. & Tech.* 2006; **3**, 13-32.
- [14] W Rittirut and C Siripatana. Diffusion properties of garcinia fruit acids (*Garcinia atroviridis*). *Walailak J. Sci. & Tech.* 2007; **4**, 187-202.
- [15] C Siripatana. Solute diffusion in fruit, vegetable and cereal processing I: Simplified solutions for diffusion in anomalous shape. *Songklanakarin J. Sci. & Technol.* 1997; **19**, 77-88.
- [16] HG Schwartzberg and RY Chao. Solute diffusivities in leaching process. *Food Technol.* 1982; **36**, 73-86.
- [17] GD Saravacos. *Mass Transfer Properties of Food*. In: MA Rao and SSH Rizvi (eds). *Engineering Properties of Foods*. 2nd ed. Marcel Dekker, New York. 1994, p. 169-221.

- [18] HG Schwartzberg. *Leaching organic materials*. In: Handbook of separation process technology. Ronald W. Rousseau (ed.). John Wiley & Sons, Inc. New York, 1987; p. 540-77.
- [19] J Spaninks. 1979, Design procedures for solid-liquid extraction. Doctoral Dissertation. Agricultural University of Netherlands, Wageningen.
- [20] W Rittirut, C Thongurai and C Siripatana. Mathematical simulation of solid-liquid diffusion in continuous-countercurrent extraction process: Part I-Modeling development. *Int. J. Chem. React. Eng.* 2010; **8(A112)**, 1-35.
- [21] W Rittirut, C Thongurai and C Siripatana. Mathematical simulation of solid-liquid diffusion in continuous-countercurrent extraction process: Part II-Modeling simulation and its application. *Int. J. Chem. React. Eng.* 2010; **8(A113)**, 1-28.
- [22] N Suparanon and C Siripatana. Solute diffusion in fruit, vegetable and cereal processing II: Simplified solutions for continuous counter-current diffusion. *Songklanakarin J. Sci. & Technol.* 1997; **19**, 89-101.